

# Synthesis of Novel Porphyrin Derivatives and Investigate their Application in Sensitized Solar Cells

Mohammed Thamer Jaafar <sup>a, b, \*</sup>, Luma Majeed Ahmed <sup>b</sup>, and Rahman Tama Haiwal <sup>b</sup>

<sup>a</sup> Department of Petroleum Engineering, College of Engineering, Kerbala University, Karbala, Iraq  
<sup>b</sup> Department of Chemistry, College of Science, Kerbala University, Karbala, Iraq

## Abstract

Solar energy has significant advantages compared to conventional sources such as coal and natural gas, including no emissions, no need for fuel, and the potential for installation in a wide range of locations with access to sunlight. In this investigation, heterocyclic derivatives were synthesized from several porphyrin derivatives (4,4',4'',4'''-(porphyrin-5,10,15,20-tetraol) tetra benzoic acid) compound (3), obtained by reaction Pyrrole with 4-formyl benzoic acid. Subsequently, porphyrin derivative-component amides 5a, 5b, and 5c were produced by reacting compound (3) with amine derivatives at a 1:4 molar ratio. These derivatives exhibited varying sensitivities for utilization in solar cells, with compound 5a displaying the highest power conversion efficiency (PCE) at 1.37%, as determined by measuring the short circuit current ( $J_{sc}$ ), open-circuit voltage ( $V_{oc}$ ), and fill factor (FF) ( $J_{sc} = 2.24 \text{ mA cm}^{-2}$ ,  $V_{oc} = 0.80 \text{ mV}$ ,  $FF = 76.5\%$ ). Meanwhile, compound 5c exhibited the lowest PCE at 0.94% ( $J_{sc} = 1.55 \text{ mA cm}^{-2}$ ,  $V_{oc} = 0.750 \text{ mV}$ ,  $FF = 76.4\%$ ).

*Keywords:* Synthesis Porphyrin, Porphyrin Derivatives, power conversion efficiency, Solar Cells.

Received on 28/02/2023, Received in Revised Form on 05/04/2023, Accepted on 06/04/2023, Published on 30/06/2023

<https://doi.org/10.31699/IJCPE.2023.2.13>

## 1- Introduction

Greek porphyria, which means purple, is the source of the term porphyrin. They belong to a vast family of highly colored pigments with a substituted aromatic macrocycle ring that is either natural or synthetic in origin and are composed of four pyrrole rings connected by four methine bridges [1–6].

The study of porphyrins has recently attracted more and more attention. porphyrins are utilized in a wide range of devices and applications, including optoelectronic, luminescent, and molecular logic ones, photonic materials, solar energy harvesting systems, supramolecular self-assembly, and medicines. The porphyrins' various electrochemical and photophysical characteristics, as well as the exocyclic substituents on the macrocycle's capacity to fine-tune these properties, have an impact on these applications [7–11].

Porphyrins have a wide variety of beneficial properties, some of which include high stability, strong photon absorption, a highly conjugated plane, and a little energy difference exists between the lowest unoccupied molecular orbital (LUMO) and highest occupied molecule orbital (HOMO). These are just a few examples of the benefits that porphyrins offer. A porphyrin has an appropriate quantity of electrons due to its highly conjugated -electron skeleton and transitions often result in substantial absorption in the UV and visible range [12–15].

Despite the abundance of described procedures, it is still difficult to synthesize porphyrins with specified functional patterns. Separations, purifications, and the scarcity of acceptable precursors all add to the challenges. Despite reports of synthetic approaches to different porphyrins, there is currently no supply of porphyrin building blocks with certain peripheral substituents [16–18].

The solar cell, a promising source of renewable energy that transforms sunlight into electricity, has great promise for helping to address humanity's ongoing energy crisis. Due to its multiple benefits, including its capability to operate in an acoustically tranquil setting, and its absence of toxicity or greenhouse gas emissions, the field of solar energy technology is currently experiencing significant expansion. As opposed to other photovoltaic devices, dye-sensitized solar cells (DSSCs) stand out among other solar cells due to their tall efficiency, inexpensive, straightforward manufacturing processes, environmental friendliness, transparency, and excellent flexibility. Although DSSCs outperform conventional solar cells in the lab, their commercial applicability is determined by factors including efficiency, longevity, and cost. Traditional DSSCs are made up of a variety of important parts, the most essential of which are a nanocrystalline semiconductor oxide, a dye sensitizer, a redox electrolyte, and a counter electrode. Traditional DSSCs also include other elements. To lower manufacturing costs and achieve excellent cell performance, in-depth research on the

individual DSSC components has recently been carried out. The performance of the cell is influenced by a variety of variables, including surface shape, particle size, TiO<sub>2</sub> photoelectrode thickness, and dye type. Utilizing liquid electrolytes, a total solar conversion efficiency of more than 12% has been attained [19–22].

However, using liquid electrolytes in DSSCs has many drawbacks, including restricted solubility of inorganic salts like KI, NaI, and LiI, electrode corrosion, and short-term stability owing to organic solvent evaporation and leakage. In order to facilitate the reduction process (I<sup>-</sup>/I<sup>-3</sup>), the counter electrode, which receives its charge from the photo-oxidized dye, injects electrons into the electrolytes. Conventional conductive glasses, such as indium- or fluorine-doped tin oxide, provide a poor rate of reduction for the counter electrode in the absence of a catalyst; as a result, the counter electrode must be coated with a catalytic substance to speed up the process. Due to its better conductivity and strong electrocatalytic activity, platinum (Pt) is favored in this respect. However, because of the corrosive I<sup>-</sup>/I<sup>-3</sup> redox electrolyte and the slow dissolution of platinum, which reduces its long-term stability, platinum is a highly costly, rare noble metal. These limitations prevent Pt electrodes from being used extensively in DSSCs. Therefore, it is crucial to create substitute noble-metal-free materials that can take the place of platinum as an electrocatalyst. It is feasible to achieve a high-power conversion efficiency with a very thin platinum film of 2 nm since the power conversion efficiency of DSSCs does not grow proportionally to an increase in the thickness of the platinum film [23–26]. As novel compounds, they have demonstrated success as photovoltaic materials by exhibiting responsiveness to solar cells. The achieved results indicate favorable prospects for utilizing newly synthesized porphyrin-based compounds in conjunction with TiO<sub>2</sub> paste as an anode material.

This work focused on the synthesis of some new substituted porphyrin derivative compounds (3) that start from Pyrrole with 4-forms benzoic acid and preparing amides derivatives from compound (3). The characterization of all prepared compounds will do and then test them as solar cells.

## 2- Experimental Part

### 2.1. Material and Instruments

The chemicals employed in this investigation were procured from a variety of manufacturers, including Sigma Aldrich, and were utilized directly without any additional purification. To verify the identity of the resulting compounds, melting points were precisely determined utilizing a digital Electro Thermal Stuart SMP-30. Fourier transform infrared spectroscopy (SHIMADZU FTIR-8400S) was conducted and reported in cm<sup>-1</sup> units. Nuclear magnetic resonance spectra were obtained in DMSO-d<sub>6</sub> using a Bruker spectrometer, operating at 500 MHz for <sup>1</sup>H NMR and 125 MHz for <sup>13</sup>C NMR. ESI-mass spectra were obtained using an Agilent

Technology (HP) instrument with electron ionization at 70 eV.

### 2.2. Preparation and Spectral Characterization of Porphyrin Derivatives

#### 2.2.1. Synthesis of 4,4',4'',4'''-(porphyrin-5,10,15,20-tetrayl) tetra benzoic acid (3)

Pyrrole (4 mol) was added to a solution of substituted aldehyde (4-formyl benzoic acid) (4 mol) in propionic acid (20 mL), and the reaction mixture was refluxed for one hour in the dark after that. After that, the solution was filtered and washed with hot water.

#### 2.2.2. Preparation of porphyrin derivatives 5a-c (General procedure)

1 mmol of SOCl<sub>2</sub> was added to 1 mmol of 4,4',4'',4'''-(porphyrin-5,10,15,20-tetrayl) tetra benzoic acid (TCPP). The mixture was stirred at 70 rpm for 30 minutes at environmental temperature, then DMF (5mL) was added with continuous stirring at the same temperature. The final solution was transferred to a round bottom flask volume (25 mL), 4 mmol of amines (a-c) were added to the last solution with reflex at 120 °C for (2-3) hours, and then 8 mmol of triethylamine (Et<sub>3</sub>N) was added with continuous reflex at 120 °C for 1huore. The black solution was added to ice crystal, filtration, and washed with ethanol.

### 2.3. Fabrication of the Working Electrodes (WE)

Isopropanol and acetone were applied to the Fluorine-doped Tin Oxide (FTO) glass slides for a total of 10 minutes to fully clean them. All cleaned substrates are then DIW washed and dried using a hot air stream. TiO<sub>2</sub> was used as an electrode in the fabrication of DSSCs, together with other photoanode materials. Every time, the paste produced from the photoanode materials was applied to the FTO substrates together with 0.2 g of TiO<sub>2</sub> with 0.4 mL of (0.1 M) HNO<sub>3</sub>, and one drop of Triton X-100 (C<sub>34</sub>H<sub>62</sub>O<sub>11</sub>, M.Wt. 646.67 g/ mol) In order to achieve the thin and symmetrical thickness indicated in Fig. 1, the produced paste is applied to an FTO-glass substrate using a glass rod. The sample is then dried for 10 minutes at 80 °C. In order to avoid dye photodegradation, the produced samples were then submerged in a porphyrin derivative-compensated amide solution for 2 hours in the dark after being annealed for 3 hours at 220 °C. The surface of the photoanode materials was cleaned with ethanol absolute to remove non-absorbed dye molecules [27]. Finally, As demonstrated in Fig. 2, the graphite electrode is created by employing a candle flame on a spotless FTO glass surface [28].

### 2.4. Preparation of the Counter Electrode (CE)

A drop of (0.1M) iodine solution was added between two prepared electrodes. A (0.1 M) iodine solution was

prepared by combining 3.175 g of iodine (I<sub>2</sub>) with 10 g of potassium iodide (KI) in 25 mL of absolute ethanol. The solution is then maintained in an opaque container after shaking the flask until the iodine has fully dissolved [29]. In order to prevent the solution from leaking beyond the designated cell region, the counter electrode is then put on the working electrode and the solution is retained in an opaque container [30].

The J-V curve was used to compute the open-circuit voltage (V<sub>oc</sub>) and short-circuit current (J<sub>sc</sub>). The following equations were used to calculate the solar cells' efficiency and fill factor (FF) [31, 32].

$$FF = \frac{J_{max} V_{max}}{J_{sc} V_{oc}} \quad (1)$$

$$\eta = \frac{J_{sc} V_{oc} FF}{I_0} \quad (2)$$

Where I<sub>0</sub> is the total incident irradiance, V<sub>max</sub> is the solar cell's maximum power point voltage, and J<sub>max</sub> is the maximum power point current.



Fig. 1. FTO Glasses Fixed with Medical Tape

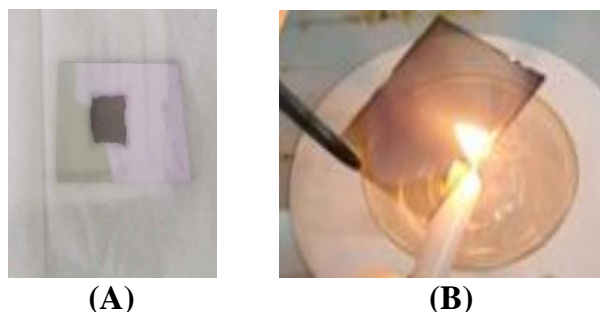


Fig. 2. (A) FTO Glasses with Dye and (B) Graphite Counter Electrode

### 3- Results and Discussion

#### 3.1. Synthesis and Spectroscopic Characterization of the Porphyrin Derivatives

The product compound (3) as shown in Fig. 3 was diagnosed using the infrared spectrum by the appearance of NH, OH, and CO groups in carboxylic acid at radii of 3371, 3300, and 1674 cm<sup>-1</sup>, respectively. The <sup>1</sup>H-NMR spectra of compound 3 showed a singlet signal at -2.29 (2H), which can be attributed to the N-H in the pyrrole group. The compound (3) was characterized by various techniques like FT-IR, <sup>1</sup>H-NMR, and Mass spectroscopy (Fig. 4 – Fig. 6).

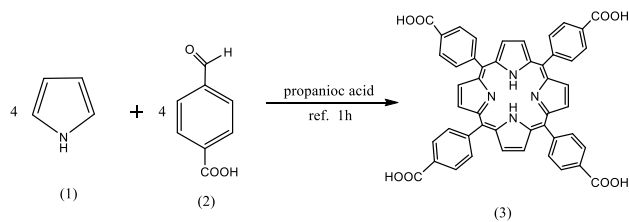


Fig. 3. Scheme of Produced of Compound (3)

(3) 4,4',4'',4'''-(porphyrin-5,10,15,20-tetra-yl) tetra benzoic acid

Color: Black powder: Yield 21%, mp > 350°C Rf =0.85 (n-hexane/ethyl acetate) FT-IR (KBr, Cm<sup>-1</sup>):3371(NH),3300-2400(OH),3043(C-H aromatic),1674(C=O), 1604 (C=N), 1573 (C=C), <sup>1</sup>H NMR (500MHz, DMSO-d<sub>6</sub>) δH (ppm): 12.91(s,4H-COOH), 8.41-8.79(d, J = 7.6 Hz Pyrrole-8H), 7.13-8.38 (m, 16 Ph-H), -2.29 (s,2NH), <sup>13</sup>C NMR (500MHz, DMSO-d<sub>6</sub>) δ C 122.25,126.64,126.92,129.53,129.55, 130.57,130.57,130.61,130.63,138.03,139.17,143.88,147.6 5,168.1 4., UV-Vis. Spectrum: (λ<sub>max</sub>), 419 nm.); EI-MS calcd exact mass (C<sub>48</sub>H<sub>30</sub>N<sub>4</sub>O<sub>8</sub>), 790.77; found, 790.6.

The second step involved the reaction of compound (3) with a variety of amines to obtain (5a-c), as explained in Fig. 7. These compounds were investigated using the infrared spectrum by disappearing the carbonyl group and appearing the amide group. The Experimental part provides all of the porphyrin derivatives' complete spectrum information (MS, FT-IR, <sup>1</sup>H, and <sup>13</sup>C NMR), as well as melting points. Compound (3) was reacted with a variety of amines in the second step to produce compound (5a-c), as displayed in Fig. 7. Using an infrared spectrum, these compounds were identified by the disappearance of the OH in carboxylic acid (3300) cm<sup>-1</sup> and the appearance of the amide group (3420) cm<sup>-1</sup>. The Experimental section gives comprehensive spectral data (MS, FT-IR, <sup>1</sup>H, and <sup>13</sup>C NMR) and melting points for all porphyrin derivatives. All the new compounds were characterized by various techniques like FT-IR and <sup>1</sup>H-NMR Mass spectroscopy (Fig. 8 – Fig. 12).

(5-a) 4,4',4'',4'''-(porphyrin-5,10,15,20-tetra-yl) tetrakis(N-benzo[d]thiazol-2-yl) benzamide

Color: Black powder: Yield 80%, mp > 350°C FT-IR (KBr, Cm<sup>-1</sup>):3420(NH Stretch),3055(C-H aromatic),1701(C=O), 1608 (C=N),1489(C=C), 636(C-S), <sup>1</sup>H NMR (500MHz, DMSO-d<sub>6</sub>): δH (ppm): 10.51 (s,4H-CONH), 8.66-8.11 (m 8H Pyrrole-H), 8.09-7.97 (m, 8 Ar-H), 7.84-7.87(m, 8 Ar-H), 7.71 (d, J = 8.1 Hz, 4H Ar-H), 7.45-7.16 (m 12H Ar-H), -2.29 (s,2NH<sub>int</sub>), <sup>13</sup>C NMR (500 MHz, DMSO-d<sub>6</sub>) δ C 120.03,120.93,122.2, 123.60,125.64,126.64,126.92,129.43,129.52,129.54,130.6 1,130.64,130.71,132.15,138.01,138.72,139.35,143.88,147 .65,150.32,156.83,159.77,166.95., UV-Vis. Spectrum: (λ<sub>max</sub>), 417nm.; Anal.Calcd for (C<sub>76</sub>H<sub>46</sub>N<sub>12</sub>O<sub>4</sub>S<sub>4</sub>): C, 69.18; H, 3.51; N, 12.74; O, 4.85; S, 9.72 found C, 69.01;

H, 3.32; N, 12.48 %, EI-MS calcd exact mass 1319.52; found, 1319.5.

72.60; H, 4.21; N, 17.70 %, ESI-MS calcd exact mass 1251.34; found, 1251.22.

(5-b) 4,4',4'',4'''-(porphyrin-5,10,15,20-tetrayl) tetrakis(N-(1H-benzo[d]imidazol-2-yl) benzamide)

(5-c) 4,4',4'',4'''-(porphyrin-5,10,15,20-tetrayl) tetrakis(N-(4-carbamoylphenyl) benzamide)

Color: Black powder: Yield 82%, mp > 350°C FT-IR (KBr,  $\text{Cm}^{-1}$ ): 3421(NH Stretch), 3036 (C-H aromatic), 1705(C=O), 1624 (C=N), 1485(C=C),  $^1\text{HNMR}$  (500MHz,  $\text{DMSO-d}_6$ ):  $\delta\text{H}$  (ppm): 11.37 (s, 4NH), 10.69 (s, 4H-CONH), 8.86-8.37 (m, 8 Pyrrole-H), 8.10-7.12 (m, 32H Ar-H), -2.25 (s, 2NH pyrrole), Anal. Calcd for ( $\text{C}_{76}\text{H}_{50}\text{N}_{16}\text{O}_4$ ): C, 72.95; H, 4.03; N, 17.91; found C,

Color: Black powder: Yield 84%, mp > 350°C FT-IR (KBr,  $\text{Cm}^{-1}$ ): 3420-3395-(NH<sub>2</sub>), 3290 (NH), 3059 (C-H aromatic), 1697(C=O), 1600 (C=N), 1484(C=C),  $^1\text{HNMR}$  (500MHz,  $\text{DMSO-d}_6$ ):  $\delta\text{H}$  (ppm): 9.84 (s, 4H-CONH), 8.67-8.64 (m, 8 Pyrrole-H), 8.15-7.31 (m, 32H Ar-H), 0693 (s, 8NH<sub>2</sub>), -1.99 (s, 2NH), Anal. Calcd for ( $\text{C}_{76}\text{H}_{54}\text{N}_{12}\text{O}_8$ ): C, 72.26; H, 4.31; N, 13.30; O, 10.13; found C, 72.02; H, 4.15; N, 13.12%.

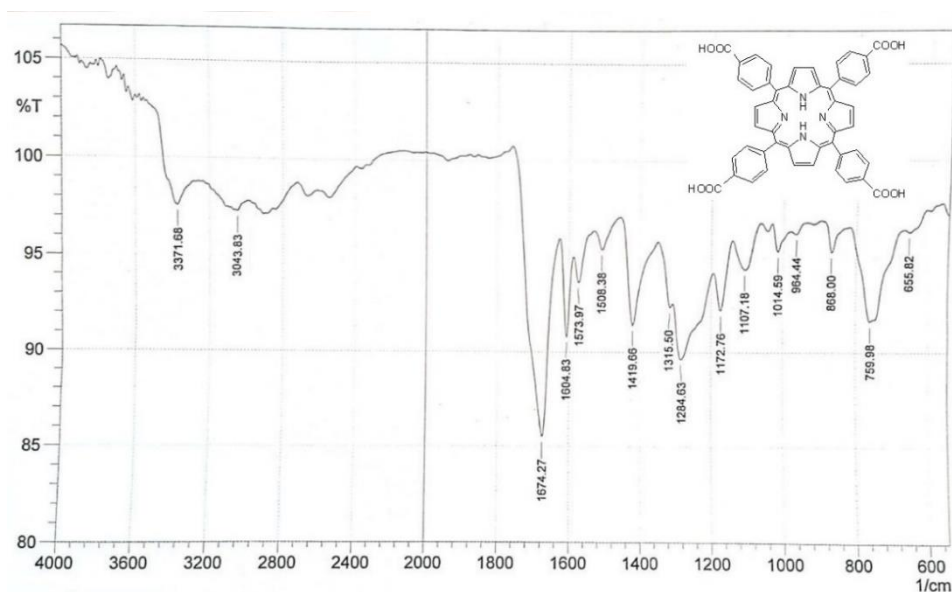


Fig. 4. FT-IR Spectrum of Compound (3)

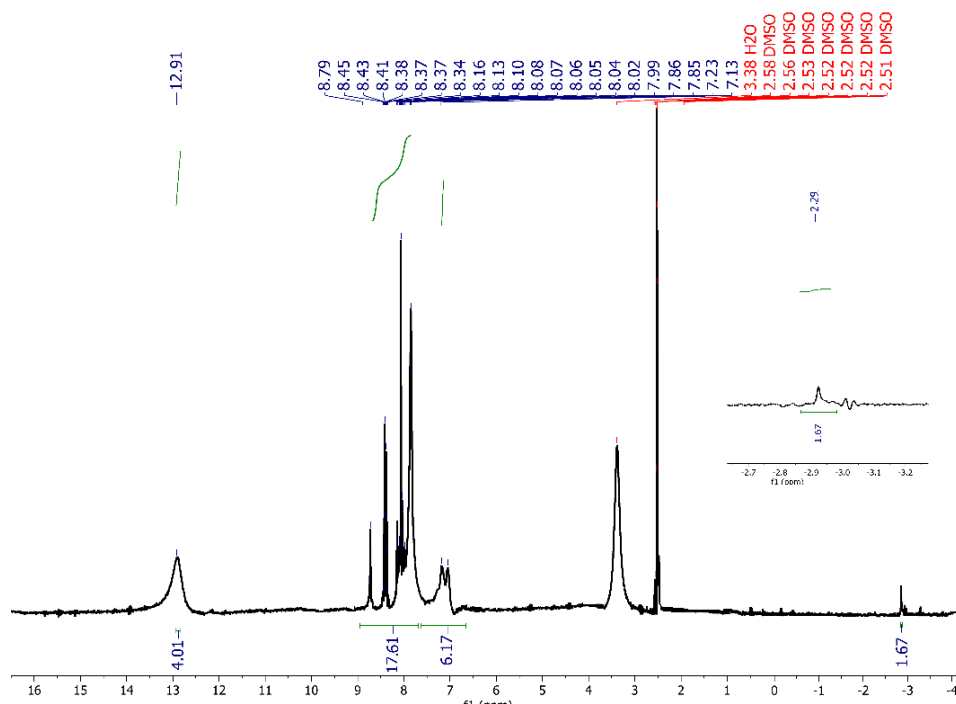


Fig. 5.  $^1\text{HNMR}$  Spectrum of Compound (3)

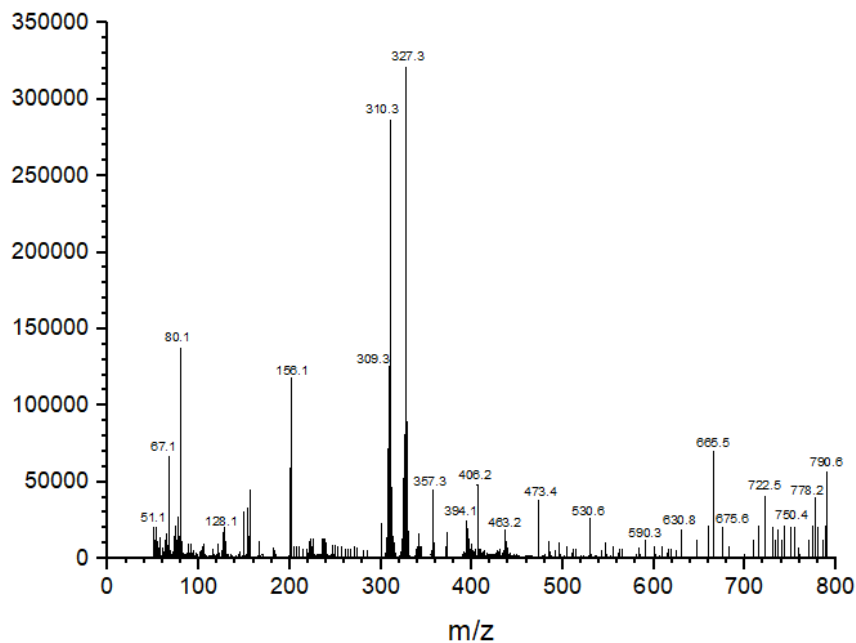


Fig. 6. Mass Spectrum of Compound (3)

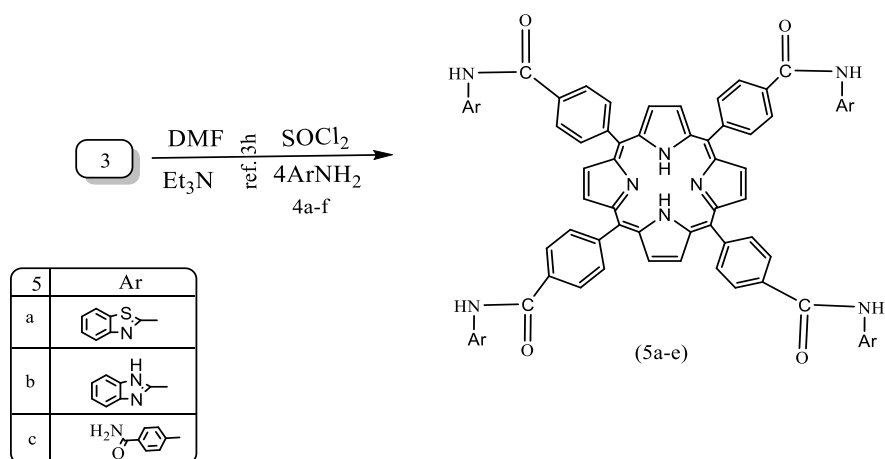


Fig. 7. Scheme of Prepared Compounds 5a, 5b, and 5c

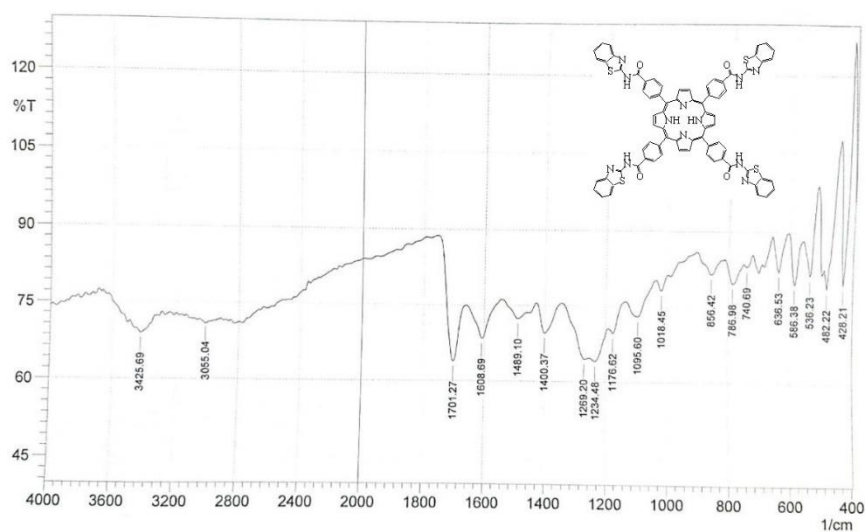


Fig. 8. FT-IR Spectrum of Compound (5a)

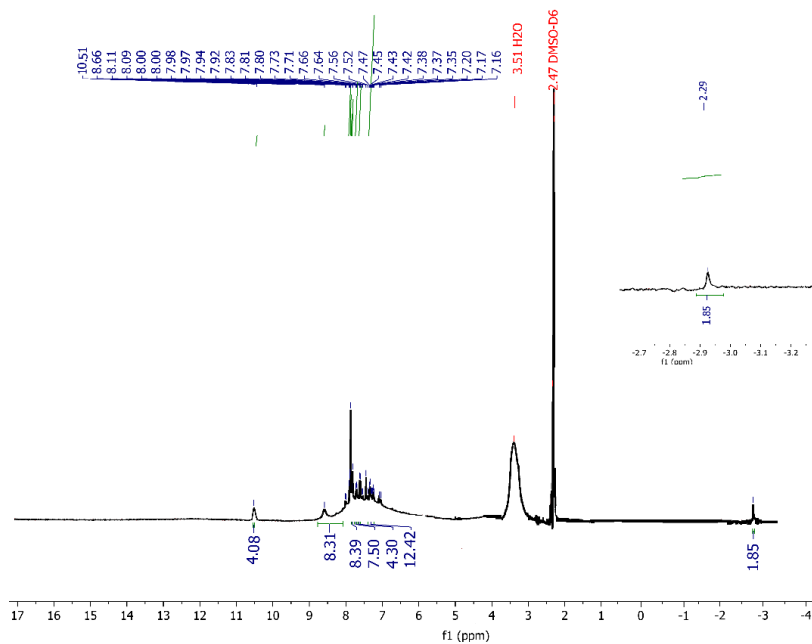


Fig. 9. <sup>1</sup>H NMR Spectrum of Compound (5a)

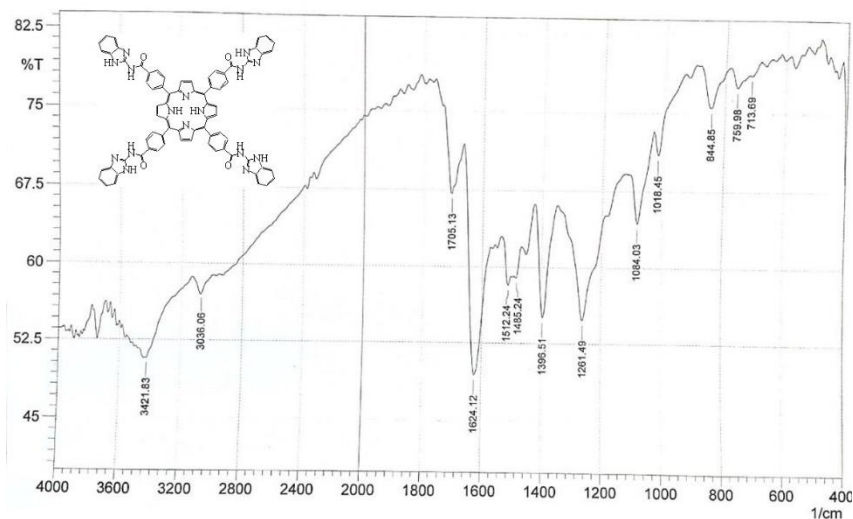


Fig. 10. FT-IR Spectrum of Compound (5b)

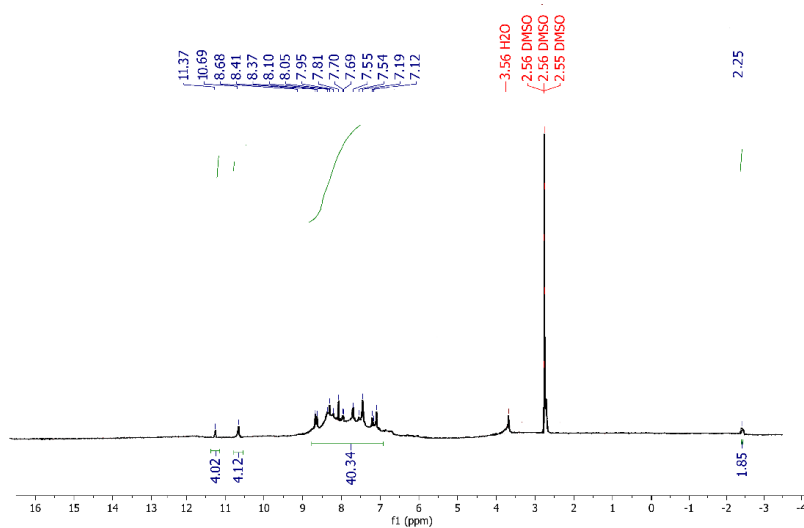


Fig. 11. <sup>1</sup>H NMR Spectrum of Compound (5b)

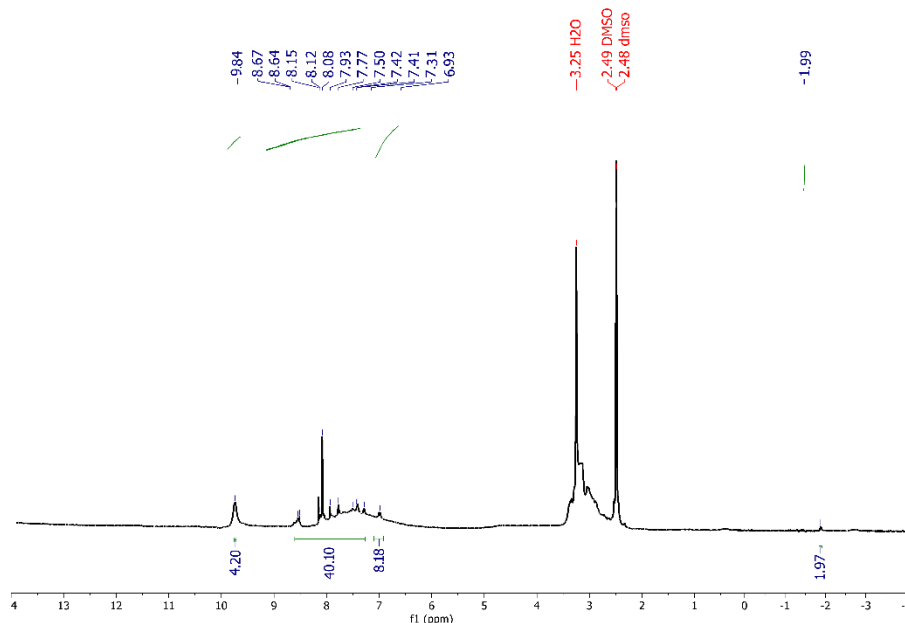


Fig. 12.  $^1\text{H}$ NMR Spectrum of Compound (5c)

### 3.2. DSSCs Test

Findings JSC,  $V_{oc}$ , FF, and PCE are shown in Fig. 13 together with the J-V curves for all produced compounds (Table 1). Based on the results in Table 1, the increased efficiencies ( $\eta$ ) for using prepared compounds are sequenced  $\eta_{5a} > \eta_{5b} > \eta_{5c}$ . The efficiency of using compound 5a is large due to have it thiazole group, which is rich in electrons (N-S) that will inject lone pair electrons to LUMO of  $\text{TiO}_2$ . On the other hand, compound 5b has an imidazole group (N-H) that has fewer lone pair electrons compared with compound 5a.

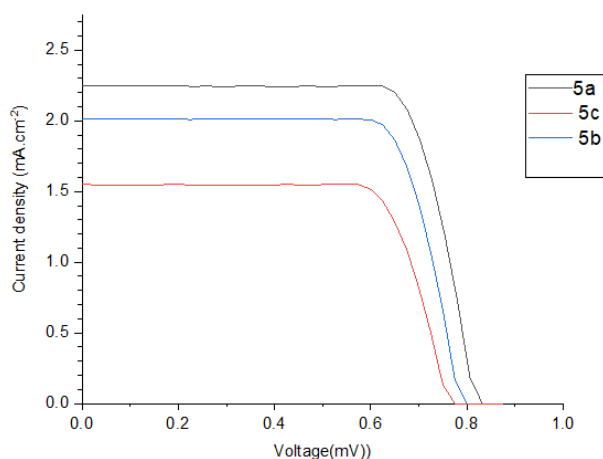


Fig. 13. J-V Curve of DSSCs Sensitized by 5a,5b and 5c

Table 1. Photovoltaic Characteristics for All Colors in a Typical Environment

Dye	$J_{sc}$ ( $\text{mA}\cdot\text{cm}^{-2}$ )	$V_{oc}$ (mV)	FF (%)	PCE (%)
5a	2.24	0.806	76.5	1.3756
5b	2.01	0.775	76.6	1.2325
5c	1.55	0.750	76.4	0.9470

### 4- Conclusion

This work is summarized:

- 1- A series of porphyrin derivatives were used as sensitized in solar cells after adsorbed on the  $\text{TiO}_2$  paste surface. This paste was poured on the FTO surface using Triton X-100 as linked material. All prepared derivatives were given the sensitivity to work as solar cells.
- 2- The maximum efficiency value was found for using derivative 5a which generates a power conversion efficiency (PCE) of 1.37%.
- 3- The 5c compound has the lowest PCE value 0.94% and that may be attributed to the smallest optical energy gap about (2.2eV) when compared to other prepared compounds.

### References:

- [1] H. Lin et al., "Preparation of Single Substituted Phenyl Porphyrins Form Meso-Tetraphenyl Porphyrin-Synthetic Example from Symmetric Porphyrin into Asymmetric Porphyrins," *Open J Inorg Chem*, vol. 08, no. 01, pp. 21–27, 2018, <https://doi.org/10.4236/ojic.2018.81002>
- [2] W. Lian, Y. Sun, B. Wang, N. Shan, and T. Shi, "Synthesis and properties of 5,10,15,20-tetrakis [4-(3,5-dioctyloxybenzamido) phenyl] porphyrin and its metal complexes," *Journal of the Serbian Chemical Society*, vol. 77, no. 3, pp. 335–348, 2012, <https://doi.org/10.2298/JSC110516190L>
- [3] P. I. Premovi, I. R. Tonsa, D. M., and M. S. Pavlovi, "Air oxidation of the kerogen/asphaltene vanadyl porphyrins: an electron spin resonance study," *Journal of the Serbian Chemical Society*, Volume 65, Issue 2, Pages: 113-121 2000. <https://doi.org/10.2298/JSC0002113P>

- [4] R. K. Lammi et al., "Structural control of photoinduced energy transfer between adjacent and distant sites in multiporphyrin arrays," *J Am Chem Soc*, vol. 122, no. 31, pp. 7579–7591, Aug. 2000, <https://doi.org/10.1021/ja001031x>
- [5] O. M. Opeyemi, H. Louis, C. I. Opara, O. O. Funmilayo, and T. O. Magu, "Porphyrin and Phthalocyanines-Based Solar Cells: Fundamental Mechanisms and Recent Advances," *Advanced Journal of Chemistry-Section A*, 2(1), 21-44 2019. <https://doi.org/10.29088/sami/AJCA.2019.2.2144>
- [6] K. Sakamoto and E. Ohno-Okumura, "Syntheses and functional properties of phthalocyanines," *Materials*, vol. 2, no. 3, pp. 1127–1179, 2009, <https://doi.org/10.3390/ma2031127>
- [7] J. L. Suk, J. T. Hupp, and S. B. T. Nguyen, "Growth of narrowly dispersed porphyrin nanowires and their hierarchical assembly into macroscopic columns," *J Am Chem Soc*, vol. 130, no. 30, pp. 9632–9633, Jul. 2008, <https://doi.org/10.1021/ja801733t>
- [8] E. Önal, "Matériaux moléculaires magnétiques à base de porphyrines," *Université Claude Bernard-Lyon I*, 2014.
- [9] H. Kim, R. Manivannan, G. Heo, J. W. Ryu, and Y. A. Son, "Porphyrin dye/TiO<sub>2</sub> entrenched in PET to attain self-cleaning property through visible light photocatalytic activity," *Research on Chemical Intermediates*, vol. 45, no. 7, pp. 3655–3671, Jul. 2019, <https://doi.org/10.1007/s11164-019-03813-4>
- [10] A. M. Shultz, O. K. Farha, J. T. Hupp, and S. B. T. Nguyen, "Synthesis of catalytically active porous organic polymers from metalloporphyrin building blocks," *Chem Sci*, vol. 2, no. 4, pp. 686–689, 2011, <https://doi.org/10.1039/c0sc00339e>
- [11] K. Zhang, Y. Yu, S. T. Nguyen, J. T. Hupp, L. J. Broadbelt, and O. K. Farha, "Epoxidation of the commercially relevant divinylbenzene with [tetrakis-(pentafluorophenyl)porphyrinato] iron(III) chloride and its derivatives," *Ind Eng Chem Res*, vol. 54, no. 3, pp. 922–927, Jan. 2015, <https://doi.org/10.1021/ie504550p>
- [12] A. Heydari-turkmani and S. Zakavi, "The first solid state porphyrin-weak acid molecular complex: A novel metal free, nanosized and porous photocatalyst for large scale aerobic oxidations in water," *J Catal*, vol. 364, pp. 394–405, Aug. 2018, <https://doi.org/10.1016/j.jcat.2018.06.011>
- [13] Y. Ding, W. H. Zhu, and Y. Xie, "Development of Ion Chemosensors Based on Porphyrin Analogues," *Chem Rev*, vol. 117, no. 4, pp. 2203–2256, Feb. 2017, <https://doi.org/10.1021/acs.chemrev.6b00021>
- [14] M. Jurow, A. E. Schuckman, J. D. Batteas, and C. M. Drain, "Porphyrins as molecular electronic components of functional devices," *Coordination Chemistry Reviews*, vol. 254, no. 19–20, pp. 2297–2310, Oct. 2010, <https://doi.org/10.1016/j.ccr.2010.05.014>
- [15] W. J. Cho, Y. Cho, S. K. Min, W. Y. Kim, and K. S. Kim, "Chromium porphyrin arrays as spintronic devices," *J Am Chem Soc*, vol. 133, no. 24, pp. 9364–9369, Jun. 2011, <https://doi.org/10.1021/ja111565w>
- [16] P. Zhang, M. Wang, C. Li, X. Li, J. Dong, and L. Sun, "Photochemical H<sub>2</sub> production with noble-metal-free molecular devices comprising a porphyrin photosensitizer and a cobaloxime catalyst," *Chemical Communications*, vol. 46, no. 46, pp. 8806–8808, Dec. 2010, <https://doi.org/10.1039/c0cc03154b>
- [17] M. Noori et al., "Tuning the electrical conductance of metalloporphyrin supramolecular wires," *Sci Rep*, vol. 6, Nov. 2016, <https://doi.org/10.1038/srep37352>
- [18] M. Adineh, P. Tahay, M. Ameri, N. Safari, and E. Mohajerani, "Fabrication and analysis of dye-sensitized solar cells (DSSCs) using porphyrin dyes with catechol anchoring groups," *RSC Adv*, vol. 6, no. 18, pp. 14512–14521, 2016, <https://doi.org/10.1039/c5ra23584g>
- [19] N. Santhanamoorthi, C. M. Lo, and J. C. Jiang, "Molecular design of porphyrins for dye-sensitized solar cells: A DFT/TDDFT study," *Journal of Physical Chemistry Letters*, vol. 4, no. 3, pp. 524–530, Feb. 2013, <https://doi.org/10.1021/jz302101j>
- [20] M. R. Samantaray et al., "Synergetic effects of hybrid carbon nanostructured counter electrodes for dye-sensitized solar cells: A review," *Materials*, vol. 13, no. 12, MDPI AG, pp. 1–34, Jun. 02, 2020. <https://doi.org/10.3390/ma13122779>
- [21] G. E. Zervaki et al., "A propeller-shaped, triazine-linked porphyrin triad as efficient sensitizer for dye-sensitized solar cells," *Eur J Inorg Chem*, no. 6, pp. 1020–1033, 2014, <https://doi.org/10.1002/ejic.201301278>
- [22] Xavier A. Jeanbourquin, Xiaoe Li, ChunHung Law, Piers R.F. Barnes, Robin Humphry-Baker, Peter Lund, Muhammad I. Asghar, and Brian C. O'Regan. Rediscovering a Key Interface in Dye-Sensitized Solar Cells: Guanidinium and Iodine Competition for Binding Sites at the Dye/Electrolyte Surface. *Journal of the American Chemical Society* 2014, 136 (20) , 7286-7294. <https://doi.org/10.1021/ja411560s>
- [23] H. Gerischer, M.E. Michel-Beyerle, F. Rebertrost, H. Tributsch, Sensitization of charge injection into semiconductors with large band gap, *Electrochimica Acta*, 13(6),1968, 1509-1515, [https://doi.org/10.1016/0013-4686\(68\)80076-3](https://doi.org/10.1016/0013-4686(68)80076-3)
- [24] S. Sharma, Bulkesh Siwach, S. K. Ghoshal, and D. Mohan, "Dye sensitized solar cells: From genesis to recent drifts," *Renewable and Sustainable Energy Reviews*, vol. 70, Elsevier Ltd, pp. 529–537, Apr. 01, 2017. <https://doi.org/10.1016/j.rser.2016.11.136>
- [25] S. Kannan Balasingam, M. Lee, M. Gu Kang, and Y. Jun, "Improvement of dye-sensitized solar cells toward the broader light harvesting of the solar spectrum," *Chemical Communications*, vol. 49, no. 15, pp. 1471–1487, Jan. 2013, <https://doi.org/10.1039/c2cc37616d>

- [26] M. R. S. A. Janjua et al., "Theoretical and Conceptual Framework to Design Efficient Dye-Sensitized Solar Cells (DSSCs): Molecular Engineering by DFT Method," *J Clust Sci*, vol. 32, no. 2, pp. 243–253, Mar. 2021, <https://doi.org/10.1007/s10876-020-01783-x>
- [27] M. Q. Lokman et al., "Enhancing photocurrent performance based on photoanode thickness and surface plasmon resonance using Ag-TiO<sub>2</sub> nanocomposites in dye-sensitized solar cells," *Materials*, vol. 12, no. 13, Jul. 2019, <https://doi.org/10.3390/ma12132111>
- [28] U. I. Ndeze, J. Aidan, S. C. Ezike, and J. F. Wansah, "Comparative performances of nature-based dyes extracted from Baobab and Shea leaves photosensitizers for dye-sensitized solar cells (DSSCs)," *Current Research in Green and Sustainable Chemistry*, vol. 4, Jan. 2021, <https://doi.org/10.1016/j.crgsc.2021.100105>
- [29] M. Halka, S. Smoleń, I. Ledwozyw-Smoleń, and W. Sady, "Comparison of Effects of Potassium Iodide and Iodosalicylates on the Antioxidant Potential and Iodine Accumulation in Young Tomato Plants," *J Plant Growth Regul*, vol. 39, no. 1, pp. 282–295, Mar. 2020, <https://doi.org/10.1007/s00344-019-09981-2>
- [30] C. Longo and M.-A. de Paoli, "Dye-Sensitized Solar Cells: A Successful Combination of Materials," 2003. <https://doi.org/10.1590/S0103-50532003000600005>
- [31] S. Umale, V. Sudhakar, S. M. Sontakke, K. Krishnamoorthy, and A. B. Pandit, "Improved efficiency of DSSC using combustion synthesized TiO<sub>2</sub>," *Mater Res Bull*, vol. 109, pp. 222–226, Jan. 2019, <https://doi.org/10.1016/j.materresbull.2018.09.044>
- [32] N. Kutlu, "Investigation of electrical values of low-efficiency dye-sensitized solar cells (DSSCs)," *Energy*, vol. 199, May 2020, <https://doi.org/10.1016/j.energy.2020.117222>

